Impact of Facility Pressure on the Wear of the NASA HERMeS Hall Thruster

IEPC-2019-714

Presented at the 36th International Electric Propulsion Conference
University of Vienna • Vienna • Austria
September 15 – 20, 2019

Jason D. Frieman[1], Hani Kamhawi[2], Peter Y. Peterson[3], and Daniel Herman[4]
NASA Glenn Research Center, Cleveland, OH, USA 44135

James Gilland[5]
Ohio Aerospace Institute
NASA Glenn Research Center, Cleveland, OH, USA 44135

and

Richard Hofer[6],
Jet Propulsion Laboratory, California Institute of Technology, Pasadena, CA, USA 91109

Abstract: This work presents an overview and summary of the results acquired during the final segment of the TDU-3 Long Duration Wear Test, which was completed in October 2018. The overall goal of this segment was to quantify the impact of facility pressure on the wear of the Hall Effect Rocket with Magnetic Shielding Technology Demonstration Unit Three (TDU-3) Hall thruster. This was accomplished by operating TDU-3 for approximately 270 hours at the nominal 600 V/12.5 kW operating condition while a bleed or auxiliary flow of xenon propellant was injected into the vacuum facility in order to raise the operating pressure to match that of another test facility in which previous wear segments had been performed. The performance, plume, stability, and wear results acquired at this elevated pressure (11.7 μTorr) are compared with equivalent data taken at the nominal operating pressure (4.2 μTorr) in the same facility as well at the elevated operating pressure in the other facility. Implications of these results for acquiring facility-independent service life estimates are discussed.

I. Introduction

NASA continues to evolve a human exploration approach for beyond low-Earth orbit and to do so, where practical, in a manner involving international, academic, and industry partners.[1] This approach is based on an evolutionary human exploration architecture, expanding into the solar system with cis-lunar flight testing including construction of the Gateway and validation of exploration capabilities before crewed missions beyond the Earth-moon system.

[1] Research Engineer, Electric Propulsion Systems Branch, jason.d.frieman@nasa.gov
[2] NASA AEPS Test Lead, Electric Propulsion Systems Branch, hani.kamhawi-1@nasa.gov
[3]Solar Electric Propulsion Deputy Project Lead Engineer, Electric Propulsion Systems Branch, peter.y.peterson@nasa.gov
[4] Solar Electric Propulsion Project Lead Engineer, Electric Propulsion Systems Branch, daniel.a.herman@nasa.gov
[5] Research Team Manager, Electric Propulsion Systems Branch, james.h.gilland@nasa.gov
[6] NASA AEPS Thruster Lead, Electric Propulsion Group, richard.r.hofer@jpl.nasa.gov

High-power solar electric propulsion is one of those key technologies that has been prioritized because of its significant exploration benefits. Specifically, for missions beyond low Earth orbit, spacecraft size and mass can be dominated by onboard chemical propulsion systems and propellants that may constitute more than 50 percent of spacecraft mass. This impact can be substantially reduced through the utilization of Solar Electric Propulsion (SEP) due to its substantially higher specific impulse. Studies performed for NASA's Human Exploration and Operations Mission Directorate and Science Mission Directorate have demonstrated that a 40-kW-class SEP capability can be enabling for both near term and future architectures and science missions.[2] In addition, a high-power, 40 kW-class Hall thruster propulsion system provides significant capability and represents, along with flexible blanket solar array technology, a readily scalable technology with a clear path to much higher power systems.

Accordingly, since 2012, NASA has been developing a Hall thruster electric propulsion string that can serve as the building block for this high-power system. The Hall thruster system development, led by the NASA Glenn Research Center (GRC) and the Jet Propulsion Laboratory, began with maturation of the 12.5-kW Hall Effect Rocket with Magnetic Shielding (HERMeS) and power processing unit. The technology development work has since transitioned to Aerojet Rocketdyne via a competitive procurement selection for the Advanced Electric Propulsion System (AEPS) contract, which includes the development and qualification of flight electric propulsion strings. The AEPS electric propulsion string consists of the 12.5-kW Hall thruster, power processing unit (including digital control and interface functionality), xenon flow controller, and associated intra-string harnesses. NASA continues to support the AEPS development by leveraging in-house expertise, plasma modeling capability, and world-class test facilities. NASA also executes AEPS and mission risk reduction activities to support the AEPS development and mission applications.

As part of these risk reduction activities, NASA has conducted a series of three wear tests to identify erosion phenomena and the accompanying failure modes as well as to validate service-life models for magnetically-shielded thrusters. These tests utilized two different technology demonstration unit (TDU) thrusters with similar designs. The first began in 2016 and accumulated approximately 1,700 hours of operation using the TDU-1 thruster.[3] The second was performed in 2017 with the TDU-3 thruster and consisted of a series of seven short duration (~200 hour) segments each testing a different thruster configuration or operating condition.[4] This test is referred to as the TDU-3 Short Duration Wear Test (SDWT) throughout this paper. The third wear test (named the TDU-3 Long Duration Wear Test or TDU-3 LDWT) began in October 2017 and was completed in October 2018.[5] The overall goal of this test was to quantify performance, stability, plume, and wear trends of TDU-3 over at least 3,000 hours of operation as a pathfinder for the planned life and qualification test of the AEPS hardware.

In addition to using two different TDU thrusters, these wear tests also consisted of segments performed in two different test facilities: Vacuum Facility 5 (VF-5) and 6 (VF-6) at NASA GRC.[4] Although both facilities are configured similarly, VF-5 has approximately twice the pumping speed of VF-6, resulting in approximately 60% lower operating pressures.[4,6] Since numerous studies have shown that facility pressure can impact Hall thruster performance, plume, and stability characteristics, it is important to determine the resultant impact of facility pressure on wear so that a facility-independent prediction of service life can be obtained from the acquired wear test data.[7–10] This work presents an overview and summary of the results obtained from the final segment of the LDWT, which had the overall goal of assessing this potential impact of facility pressure on wear.

II. Summary of the Long Duration Wear Test

The TDU-3 LDWT accumulated approximately 3,570 hours of total operating time split between six wear segments. A summary of these segments is shown Table 1.

Segment I was performed at the nominal TDU operating condition of 600 V/12.5 kW and resulted in the accumulation of 1015 hours of operating time. This segment was interrupted by a facility anomaly and so was completed in two consecutive parts lasting 620 h and 395 h, respectively. The elevated facility pressure measured during this segment was most likely due to initial outgassing and bake out of the carbon panels lining the facility walls. This is supported by the fact that the facility operating pressure was observed to decrease from approximately 8 μTorr to 4 μTorr over the course of this segment.

Segments II-IV were all performed at the 300 V/6.25 kW throttle point, however, each was performed at a different magnetic field strength. Segment II was performed at the nominal magnetic field strength (1 B) while Segments III and IV were performed at field strengths of 0.75 B and 1.5 B. Each of these segments lasted for between 200 and 250 hours and has been detailed in previous work.[5]

Segment V was performed at the nominal TDU operating condition of 600 V/12.5 kW and resulted in the accumulation of 1579 hours of operating time with a carbon-carbon (C-C) composite inner front pole cover (IFPC).

This was done in order to assess the lifetime of an alternate pole cover material with increased strength and crack resistance. This segment was interrupted by three anomalies and so was completed in four consecutive parts lasting approximately 555 h, 241 h, 380 h, and 403 h, respectively. The results of this segment are discussed in detail in previous work.[11]

The focus of this work is on Segment VI, which was also performed at the 600 V/12.5 kW operating condition. However, unlike Segments I and V, Segment VI was performed at an elevated facility pressure of approximately 11.7 µTorr in order to match the nominal operating pressures observed for wear segments performed in VF-6.

Table 1 TDU-3 LDWT Test Segments.

Segment	I	II	III	IV	V	VI
Operating Condition*	600 V/1 B	300 V/1 B	300 V/0.75 B	300 V/1.5 B	600 V/1 B	600 V/1 B
Facility Pressure (µTorr)	5.7	4.2	4.1	4.2	4.3	11.7
Segment Duration (h)	1015	252	214	240	1579	270

*All segments completed at a discharge current of approximately 20.8 A in VF-5.

III.Experimental Apparatus

A. HERMeS Thruster

All LDWT segments were performed using the 12.5-kW NASA HERMeS TDU-3. The overall HERMeS design incorporates technologies developed by NASA over nearly two decades, including a magnetic shielding topology to eliminate discharge channel erosion as a life-limiting mechanism. The result is a significant increase in the operational lifetime of state-of-the-art HETs, with HERMeS being designed to operate at a specific impulse of 3,000 s for an operational lifetime exceeding 50 kh.[12–16]

The HERMeS TDU-3 thruster is shown in the configuration used for the majority of the LDWT in Figure 1. The thruster configuration was largely unchanged from that used during the previous TDU-3 SDWT, with two exceptions.[4] First, a pair of new magnet coils were installed in TDU-3 prior to the LDWT. This resulted in a change in the current settings required to achieve a fixed magnetic field strength, but did not change the magnetic field shape.

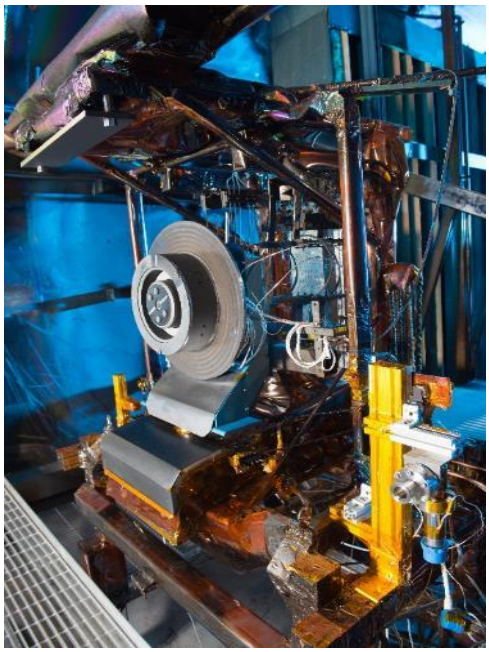

Figure 1. HERMeS TDU-3 Hall thruster in the configuration used for the LDWT.

The second exception was the position and thickness of the cathode keeper. During the TDU-1 wear test, the cathode keeper was positioned upstream of the IFPC.[3,4] During the TDU-3 SDWT, changes to the design of the IFPC resulted in a keeper position that was coplanar with the downstream surface of the IFPC; this represents a downstream shift relative to the TDU-1 position by a distance approximately equal to the thickness of the IFPC.[4] For the TDU-3 LDWT, the cathode was returned to the position used during the TDU-1 wear test (i.e., upstream of the IFPC) and the segments of the SDWT performed in VF-6.[4,5] In addition, the keeper thickness was doubled during the LDWT to provide added lifetime margin. The impacts of these keeper changes are discussed in previous work.[5] The same cathode (here defined as heater, tube, and insert) was used for all 3 TDU wear tests.

Although the cathode position used during the LDWT matches that used during the TDU-1 wear test, a number of other small design changes differentiate TDU-3 and TDU-1 including a change in the grade of boron nitride used for the discharge channel. A detailed description of these changes is provided in Kamhawi et al. [13]; the results from that work suggest they resulted in minimal changes to HET performance, stability, and plume properties

B. Thruster Support Equipment

Xenon propellant was supplied to the thruster and the centrally-mounted cathode using a laboratory feed system composed of stainless-steel lines metered with commercial thermal mass flow controllers. The anode line was metered

using a 500-sccm controller, and the cathode line was metered using a 100-sccm controller. All controllers were calibrated before and after the test using a NIST-traceable piston prover. The controllers had a measured uncertainty of approximately 1 sccm for the anode and 0.2 sccm for the cathode.[17] This system was identical to that used in previous TDU wear tests.[3,4]

All power to TDU-3 was provided using a power console composed of commercial laboratory power supplies. The discharge was controlled using three 15-kW (1000 V, 15 A) power supplies connected in a master-slave configuration. The output from these supplies was connected to a laboratory wire harness with an inductance and capacitance of approximately 2.5 µH and 236 pF, respectively.[18] This console was equipped with a set of safety interlocks that allows the data acquisition or vacuum facility control system to disable power and place the thruster in a safe state in the event that a facility or thruster anomaly is detected. This setup was unchanged from previous HERMeS characterization and wear tests.[3,4,9,13,19,20]

Following the results from the electrical configuration study performed by Peterson et al.[20], the TDU-3 thruster body was electrically tied to the cathode, and all conductive surfaces within approximately one meter of the thruster exit plane were insulated using dielectric sheeting.[20,21] This was done in order to provide better control over the number of electrical coupling paths between the HET and facility in the near-field.[20,21]

Thruster telemetry was recorded continuously at a rate of approximately 0.5 Hz using a multiplexed data acquisition system. End-to-end calibrations of the laboratory power and data acquisition systems (DAQ) were performed before and after the test using a NIST-traceable digital multimeter. The resultant uncertainty was approximately ±0.06 V and ±0.03 A for measurements of voltage and current, respectively. Nearly all voltages were measured both at the breakout box (BoB) and via a sense line at the interface between TDU-3 and the facility cable harness. Unless otherwise noted, all voltages reported in this work correspond to the measurements from the sense lines.

Three oscilloscopes were used to monitor oscillations during the LDWT. The first two oscilloscopes were used to compute the root-mean-square (RMS) and peak-to-peak values of the discharge current, discharge voltage, cathode-to-ground voltage, keeper voltage, and body voltage. These measurements were obtained over intervals of 100,000 samples at a sampling rate of 1 MS/s and recorded by the DAQ. The final oscilloscope was used to obtain waveforms of the AC components of the discharge current, discharge voltage, and keeper voltage. These waveforms consisted of 5 million points sampled at a rate of 50 MS/s. All oscillation data reported in this work were collected using this third oscilloscope. For all three oscilloscopes, current measurements were acquired using 150-A AC/DC current probes while voltage measurements were acquired using high-voltage differential probes.

C. Vacuum Facility

All experiments detailed in this work were performed in VF-5 at NASA GRC. VF-5 is a cylindrical chamber measuring 4.6 m in diameter and 18.3 m in length.[22] For this test, VF-5 was evacuated using a series of cryopumps. The cryopumps have a total effective pumping area of 33.5 m^2 and a combined nominal pumping speed of approximately 700,000 l/s on xenon.[22–24] In order to obtain the lowest possible background pressure, the thruster was installed in the main volume of VF-5 at the same location as in previous wear tests, as shown in Figure 2. [3,4] The placement of the cryopumps relative to the thruster at this location as well as the resultant near-field background neutral distribution is described in previous work. [22–24]

Facility pressure was monitored with two xenon-calibrated and one nitrogen-calibrated Bayard-Alpert style hot-cathode ionization gauges. One xenon-calibrated gauge (SIG 3 Xe) was centered approximately 0.7 m radially outward, 0.08 m upstream, and 0.6 m below the HET exit plane. The orifice of SIG 3 Xe faced radially outward (i.e., away from the HET). The second xenon-calibrated gauge (SIG 2 Xe) was mounted adjacent to and downstream of SIG 3 Xe and had a downstream-facing orifice. It is important to note that SIG 2 Xe was replaced with the equivalent gauge from VF-6 prior to the start of Segment VI. This was done in order minimize gauge-to-gauge uncertainty when comparing the elevated pressure achieved in VF-5 with the nominal operating pressure of VF-6. The nitrogen-calibrated gauge (SIG 2 N_2) was located approximately 0.7 m radially outward, 0.05 m upstream, and 0.4 m below the HET exit plane. The orifice of SIG 2 N_2 faced radially outward.

All ion gauges used in this work were configured for operation with electric propulsion systems and thus had an elbow and plasma screen installed on the inlet of the gauge.[25] The housing of each gauge was also attached to facility ground via an electrical grounding strap to avoid charging effects. A thermocouple was installed on the exterior of each ion gauge tube; this allowed the measured pressures to be corrected for thermal effects.[26] The gauge temperatures and pressures were sampled using the same multiplexed DAQ used to record thruster telemetry.[25] Consistent with previous tests performed in VF-5, all pressures reported in this work correspond to the measurements made using SIG 3 Xe.[3,4,9,13,19,20]

In order to raise the operating pressure during Segment VI, a bleed or auxiliary flow of xenon was injected into VF-5 through a pair of orifices installed near the bottom of the facility. As shown in Figure 2, the first orifice was

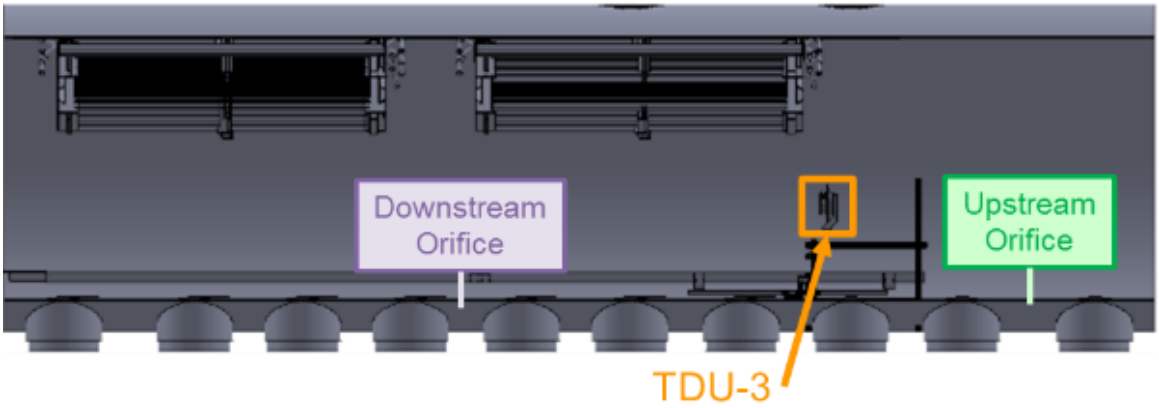

Figure 2. Locations of bleed flow orifices used during Segment VI of the TDU-3 LDWT.

installed downstream of TDU-3 at approximately the mid-point of the facility. This position is identical to the one used during the TDU-1 Facility Effect Characterization Test (FECT).[9] The second was installed between the two cryopanels located upstream of TDU-3. In order to avoid artificially introducing bulk neutral motion, both orifices were equipped with diffusers and a barrier to prevent flow injection towards the thruster.[7] During Segment VI, the bleed flow rates through each orifice were varied until the ion gauges facing radially (i.e., SIG 2 Xe) and downstream (SIG 3 Xe) both read approximately 11 μTorr. This was done in order to provide the closest analog to the near-field backpressure environment observed for TDU operation in VF-6.[6]

D. Diagnostics

1. Thrust Stand

Thrust was measured using the same null-type inverted pendulum thrust stand used in previous HERMeS performance characterization and wear tests.[3,4,9,13,19,20] The design and theory of operation of the thrust stand are detailed in several previous works.[27–29]

During the LDWT, the thrust stand was operated in a null-coil configuration. In this configuration, the position of the thruster is measured by a linear variable differential transformer (LVDT) and maintained by a pair of electromagnetic actuators. The current through each actuator is controlled using an integral-differential controller that uses the LVDT signal as the input and then modulates the current through the actuators in order to hold the thruster stationary. The thrust is then correlated to the resultant current through one of these actuators (i.e., the null coil). The thrust stand is also equipped with a closed-loop inclination control circuit, which uses an integral controller and piezoelectric actuator to maintain the inclination measured by an electrolytic tilt sensor and thus minimize thermal drift during performance measurements.

The thrust stand was calibrated before each performance characterization period by loading and offloading a set of known weights using an in-situ pulley system. All reported thrust measurements have been corrected for thermal drift and offsets from the desired discharge power. The resultant thrust stand uncertainty for this work is approximately ± 5 mN.[30]

2. Plasma Diagnostics

Plume measurements were made using a probe suite containing a Faraday probe (FP), Langmuir probe (LP), retarding potential analyzer (RPA), and a Wien filter spectrometer (WFS or ExB probe). All probes were mounted in a single array attached to a remotely operated stage system that allowed for rotational and radial motion of the probes to precise angular and radial positions in the plume. These diagnostics have been used in previous HERMeS characterization and wear tests and are further detailed in Huang et al.[9]

E. Erosion Measurements

1. Profilometer

All erosion measurements were made with a chromatic, white-light non-contact benchtop profilometer. The employed profilometer is equipped with an optical pen oriented normal to the HET exit plane with a 3-mm measuring range. All acquired profilometry data were analyzed according to the guidance established in the ISO 5436-1 measurement standard for a type A1 step (i.e., a wide groove with a flat bottom).[31] Uncertainty was quantified using the technique detailed by Mackey et al. [32] that accounts for instrument error, surface roughness, wear due to operation at points other than the nominal wear point, and the non-flat nature of the acquired profiles. The results of this uncertainty analysis yielded typical uncertainties on the order of ±2 μm for this work.

2. Wear Surface Configuration

Similar to the approach taken in previous HERMeS wear tests, the inner front pole cover (IFPC), outer front pole cover (OFPC), and keeper were modified in order to better characterize component erosion rates.[3,4] In order to minimize the variation in pre-test surface roughness and thus provide as uniform a baseline as possible, each of these surfaces was polished prior to installation. In addition, graphite masks were installed to provide unexposed surfaces to use as a reference for post-test analysis. Two 0.5-mm thick graphite masks were installed at the 2 o'clock and 8 o'clock locations of the IFPC. These masks are shown in Figure 3(a) and are identical (in both dimension and location) to the graphite masks used during previous segments of the LDWT as well as the SDWT.[4,5]

Segment VI of the LDWT reused the graphite OFPC from Segment IV.[5] As shown in Figure 3(b), the 3 to 4 o'clock region of this OFPC was polished pre-test. Two masks were installed over the polished region at the 3 and 4 o'clock positions. An additional mask was installed over the unpolished region of OFPC at the 10 o'clock position. It is important to note that this is the only pole cover used during the LDWT in which a previously exposed region of the pole cover was re-polished between test segments and that the mask at 10 o'clock was installed over a region of the pole cover that was never polished.

The keeper configuration used during the TDU-3 LDWT is shown in Figure 3(a). The keeper was made of graphite and had the downstream surface polished prior to installation. A graphite ring was affixed to the outer edge of the downstream keeper face. This ring increased the diameter of the keeper to match the AEPS design and provided a masked reference surface for keeper erosion measurements. A small tab was also included as part of the mask, which protruded radially inwards towards the cathode orifice. This tab enabled an assessment of the radial variation in erosion rates across the keeper face. Segment VI reused the keeper from Segment V, but the mask was rotated prior to the start of Segment VI to expose a new region of polished graphite. This enabled direct measurements of the keeper wear for both segments.

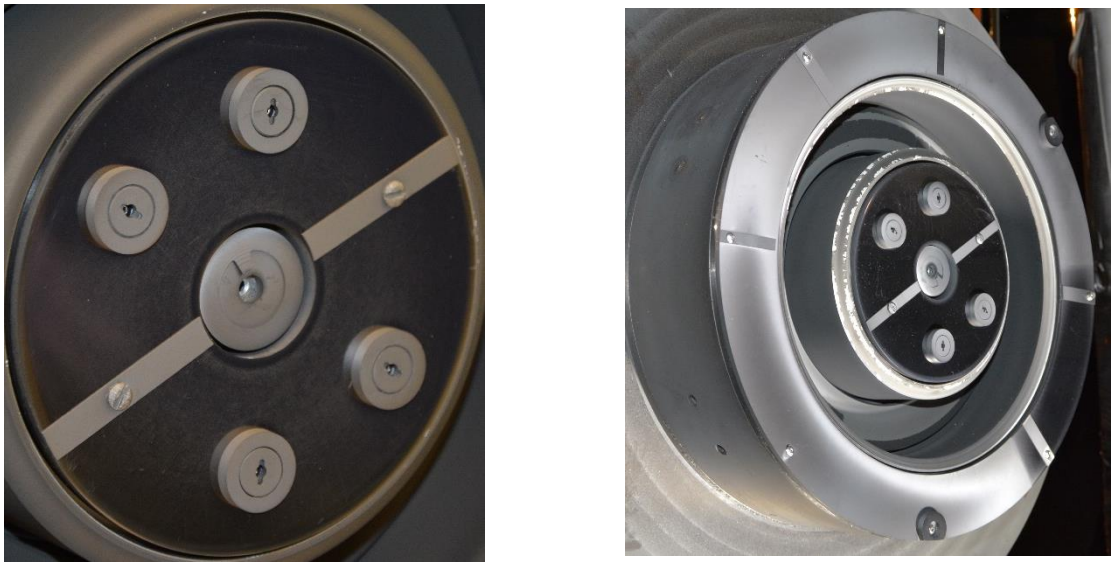

(a) (b)

Figure 3. (a) IFPC and (b) OFPC configuration used during Segment VI of the TDU-3 LDWT.

Table 2 Reference firing conditions used during the TDU-3 LDWT.

RFC	Discharge Voltage (V)	Discharge Current (A)	Discharge Power (W)
1	300	9.00	2700
2	300	20.83	6250
3	400	20.83	8333
4	500	20.83	10417
5	600	20.83	12500
6	630	20.83	13123

IV. Results

As in previous wear tests, continuous operation at each of the segments listed in Table 1 was periodically interrupted in order to acquire performance, stability, and plume data for the reference firing conditions shown in Table 2. It is important to note that, even during Segment VI, these reference firings were performed at the nominal operating pressures for VF-5 before returning to elevated pressure. During the LDWT, these average facility pressures were approximately 3 µTorr-Xe for operation at RFC 1 and 4.5 µTorr-Xe for all other conditions.

A. Performance and Stability

The thrust and anode flow rate for RFC 5 measured during the LDWT are shown as a function of facility pressure in and Figure 4(a) and (b), respectively. Also included in Figure 4 are the results from the FECT performed using TDU-1 in VF-5 and detailed in Huang, et al.[9] Consistent with results from the FECT, the thrust of TDU-3 changed by less than the empirical uncertainty across the range of tested pressures during Segment VI of the LDWT. Furthermore, the thrust and anode flow rate matched those obtained in VF-6 at similar operating pressures.

As discussed in Section III.C, the configuration of bleed flow orifices used during the LDWT differs from that used during the TDU-1 FECT. Specifically, only the downstream orifice shown in Figure 2 was used during the TDU-1 FECT, while flow was bled in at equal rates through both the downstream and upstream orifices during the LDWT.[9] To determine the possible impact of bleed flow orientation on thruster operation, the performance of TDU-3 was measured as flow was bled in through the upstream orifice only (matching the TDU-1 FECT configuration), the downstream orifice only, and both orifices equally (matching the LDWT configuration). In all cases, the bleed flow rate was set to yield an operating pressure of approximately 11 µTorr as measured by SIG 3 Xe. Overall, these results suggest that the choice of bleed flow orifice did not impact thruster performance to within the experimental uncertainty.

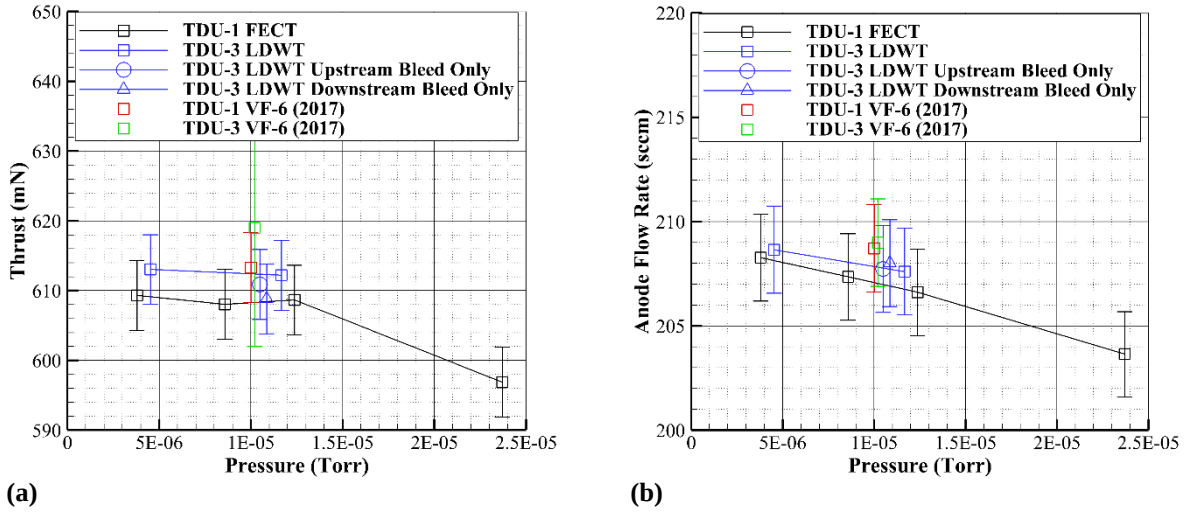

Figure 4. (a) Thrust and (b) anode flow rate as a function of facility pressure for RFC 5 (600 V/12.5 kW).

In addition to average performance, magnet maps were also acquired at both the nominal and elevated VF-5 operating pressures during Segment VI of the TDU-3 LDWT. The results are shown in Figure 5. Consistent with the performance results in Figure 4, the thrust of TDU-3 at each magnetic field strength and elevated pressure changed by less than the empirical uncertainty relative to the results obtained at nominal pressures.

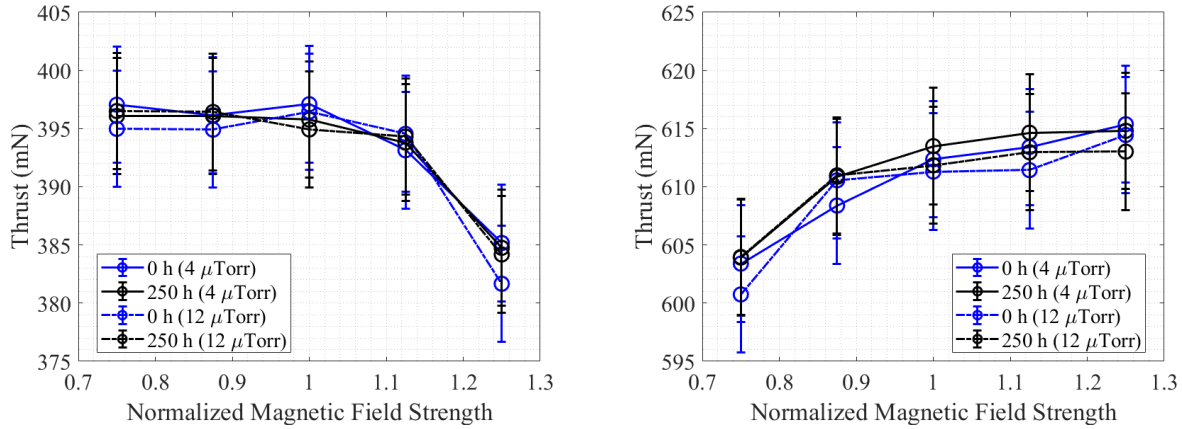

Figure 5 Thrust of TDU-3 as a function of magnetic field strength at nominal and elevated facility pressure for (a) RFC 2 (300 V/6.25 kW) and (b) RFC 5 (600 V/12.5 kW).

The impact of facility backpressure on discharge current oscillation characteristics is shown in Table 3. It is important to note that the values shown for operation at nominal facility pressure represent the average and standard deviation of all measurements taken throughout the LDWT, while those shown for operation at elevated pressure represent the average from the measurements taken during Segment VI. As shown in Table 3, operation at elevated pressure resulted in larger average discharge current peak-to-peak, RMS, and standard deviation values for RFCs 2-6. However, most of these changes were less the standard deviation and all are within the range of values measured at nominal pressures during the LDWT. This seeming invariance in oscillation statistics with pressure is consistent with the IVBs of the normalized discharge current RMS shown in Figure 6.

It is important to note that, although pressure minimally affected the statistics of the discharge current oscillations, changes were observed in the power spectral densities. Specifically, as shown in Table 3, the power and frequency associated with the second and third spectral peaks increased with operating pressure for RFCs 4, 5, and 6, while the same quantities decreased for the first spectral peak. All of these changes exceeded two standard deviations of the values measured at nominal pressures during the LDWT. Furthermore, this overall trend matches previous measurements obtained using high-speed imaging during the TDU-1 FECT.[9]

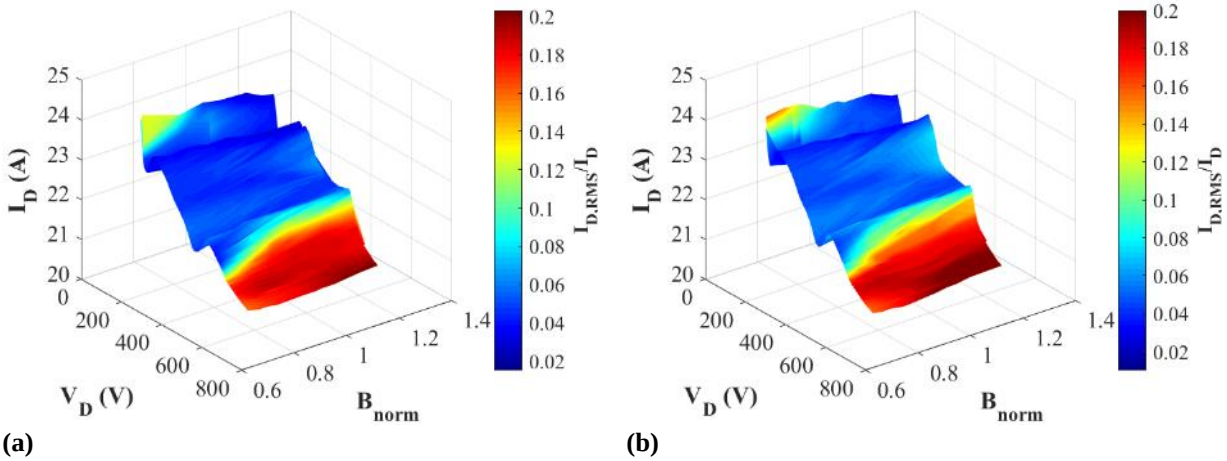

Figure 6 IVBs for operation at approximately 20 mg/s of anode flow measured at (a) nominal and (b) elevated facility pressure.

Table 3. Average peak frequencies (*f*) and power density (PD) of the TDU-3 discharge current at nominal and elevated facility pressure.

RFC	P (μTorr)	Peak 1		Peak 2		Peak 3		Statistics		
		f (kHz)	PD (dB/Hz)	*f* (kHz)	PD (dB/Hz)	*f* (kHz)	PD (dB/Hz)	Pk2Pk (A)	RMS (A)	σ (A)
1	2.5	6.4 ± 0.4	16.7 ± 1.6	-	-	-	-	1.6 ± 0.1	0.2 ± 0.01	0.2 ± 0.01
300 V, 2.70 kW	5.0	7.5	15.3	-	-	-	-	1.5	0.2	0.2
2	4.8	4.3 ± 0.2	32.8 ± 1.2	51.2 ± 2.4	17.8 ± 1.1	-	-	7.6 ± 0.3	0.9 ± 0.01	0.9 ± 0.01
300 V, 6.25 kW	11.1	4.3	32.7	51.6	17.5	-	-	8.6	1.0	1.0
3	4.7	8.0 ± 0.4	24.4 ± 1.0	69.0 ± 2.1	22.7 ± 1.1	-	-	5.6 ± 0.4	0.7 ± 0.01	0.7 ± 0.01
400 V, 8.33 kW	11.0	8.6	25.2	72.0	18.5	-	-	6.7	0.7	0.7
4	4.6	22.1 ± 0.3	45.2 ± 1.3	44.7 ± 1.7	33.2 ± 1.3	-	-	17.1 ± 0.7	3.5 ± 0.1	3.5 ± 0.1
500 V, 10.42 kW	11.1	22.7	40.6	52.8	39.3	-	-	17.6	3.5	3.5
5	4.5	15.8 ± 0.9	32.9 ± 1.4	48.9 ± 0.7	46.9 ± 1.3	98.3 ± 0.7	28.4 ± 0.8	16.6 ± 0.7	3.7 ± 0.1	3.7 ± 0.1
600 V, 12.50 kW	11.7	13.1	27.5	50.8	48.7	101.9	30.9	17.2	3.9	3.9
6	4.6	13.5 ± 1.2	30 ± 1.4	49.3 ± 0.4	48.8 ± 1.6	99.0 ± 0.8	30.2 ± 1.0	16.7 ± 0.6	3.8 ± 0.1	3.8 ± 0.1
630 V, 13.12 kW	11.2	10.5	25.8	51.5	49.5	103	32.1	17.2	4.0	4.0

B. Plume Properties

The impact of facility pressure on charge-weighted divergence angle, ion beam current, maximum high-energy polar angle, and most-probable voltage is shown for operation at 300 V and 600 V in Table 4. These values are defined and computed per the methods outlined by Huang et al.[9] Overall, changes in these plume properties were found to be smaller than 5% for operation at elevated pressure relative to the mean value measured throughout the remainder of the LDWT.

Table 4 Plume properties measured during the TDU-3 LDWT at nominal and elevated facility pressure.

Parameter	RFC 2 (300 V/6.25 kW)		RFC 5 (600 V/12.5 kW)	
	4.8 µTorr	11.1 µTorr	4.5 µTorr	11.7 µTorr
Charge-Weighted Divergence Angle (º)	24.9 ± 0.9	23.9	19.7 ± 0.3	19.8
Ion Beam Current (A)	17.9 ± 1.1	19.3	18.9 ± 0.7	19.0
Most-Probable Voltage (V)	290.0 ± 3.7	282.0	578.6 ± 19.8	576.8
High-Energy Polar Angle (º)	87.1 ± 3.8	92.5	71.3 ± 2.7	75.0

C. Wear

1. *Inner Front Pole Cover*

The impact of facility pressure on measured IFPC erosion rates for operation at the 600 V/12.5 kW operating condition are shown in Figure 7. Except at the edges of the IFPC, the erosion rates measured in VF-5 at 11 µTorr largely match those measured at 4-6 µTorr to within the measurement uncertainty. However, as shown in Figure 7, these rates are an average of 54% smaller than those measured in VF-6 during the SDWT at an equivalent background pressure and thruster operating condition.[4]

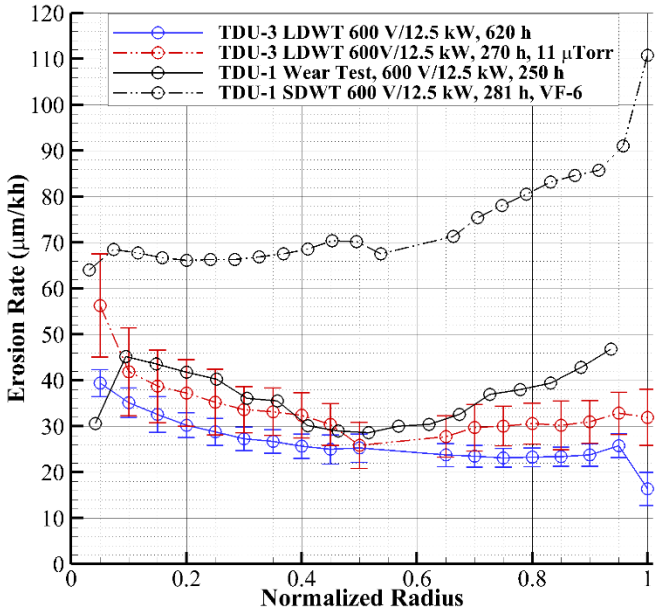

Figure 7 Impact of facility pressure on measured IFPC erosion rates for operation at 600 V/12.5 kW.

2. *Outer Front Pole Cover*

The impact of facility pressure on measured OFPC erosion rates for operation at the 600 V/12.5 kW operating condition are shown in Figure 8. Consistent with the results for the IFPC, the erosion rates measured in VF-5 at 11

µTorr largely match those measured at 4-6 µTorr to within the measurement uncertainty. The larger uncertainty of the OFPC measurements relative to those of the IFPC is primarily due to the lower erosion rate, and thus smaller step sizes, measured on the OFPC. Taken together with the results of the IFPC, this suggests that the impact of facility pressure on wear is unclear and cannot solely explain the difference in wear rates measured in VF-5 and VF-6.

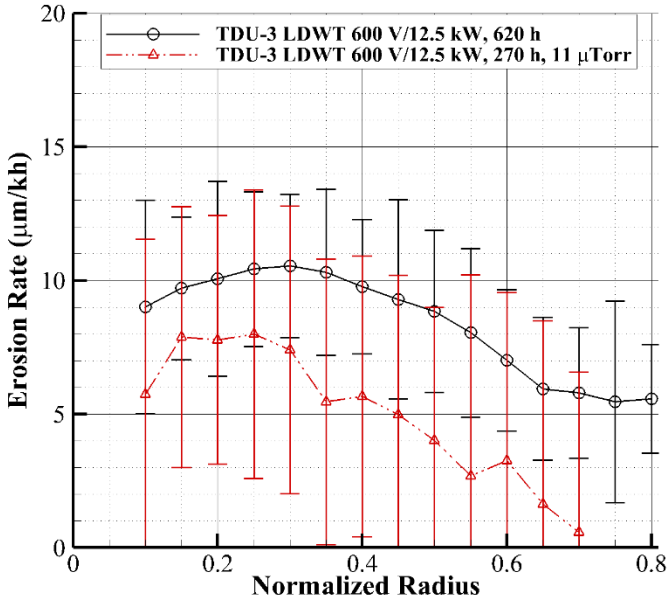

Figure 8. Impact of facility pressure on measured OFPC erosion rates for operation at 600 V/12.5 kW.

3. Cathode Keeper

The impact of facility pressure on measured keeper erosion rates for operation at the 600 V/12.5 kW operating condition are shown in Figure 9. It is important to note that all data plotted in Figure 9 were acquired in VF-5 with the cathode in the same axial location (i.e., upstream of the IFPC). Overall, the measured erosion rates at elevated pressure are 152% greater, on average, than those measured at nominal pressure. Although these variations are less than the empirical uncertainty for many radii, the overlap in error bars is small, indicating a lower probability that no change was observed. Since minimal changes were observed in cathode performance and stability parameters for operation at elevated pressure, the cause for the observed increase in keeper erosion is unclear and will require additional work in order to determine the responsible mechanism.

V.Summary and Conclusions

This work presented an overview of the results obtained from the final segment of the LDWT during which an auxiliary flow of propellant was used to purposely raise the facility pressure to match that achieved in another facility. This was done to assess the impact of pressure on performance, stability, plume properties, and, for the first time, component wear of the HERMeS TDU-3 thruster so that a facility-independent prediction of service life can be obtained.

Performance and stability of TDU-3 varied by less than the empirical uncertainty between operation at 4 µTorr and 11 µTorr. The exception was in the power spectral densities measured for operation at 500 V, 600 V, and 630 V. Here the power and frequency associated with the second and third spectral peaks increased with operating pressure. Both results match previous measurements obtained during the HERMeS Facility Effects Characterization Test.

Pole cover erosion rates measured in VF-5 at 11 µTorr largely matched those measured at 4-6 µTorr to within the measurement uncertainty. However, the IFPC erosion rates were an average of 54% smaller than those measured in VF-6 during the SDWT at an equivalent background pressure and thruster operating condition. Keeper wear increased for higher pressure, although the increase only slightly exceeded the measurement uncertainty and was accompanied by no changes in cathode performance and stability parameters (e.g., cathode-to-ground voltage, keeper voltage, etc.). Taken together, this suggests that factors other than facility pressure play a role in determining wear rates and motivates additional work to determine the responsible mechanism for the variations in erosion rates measured between facilities as well as understand how that mechanism impacts orbital service life predictions made using ground test data.

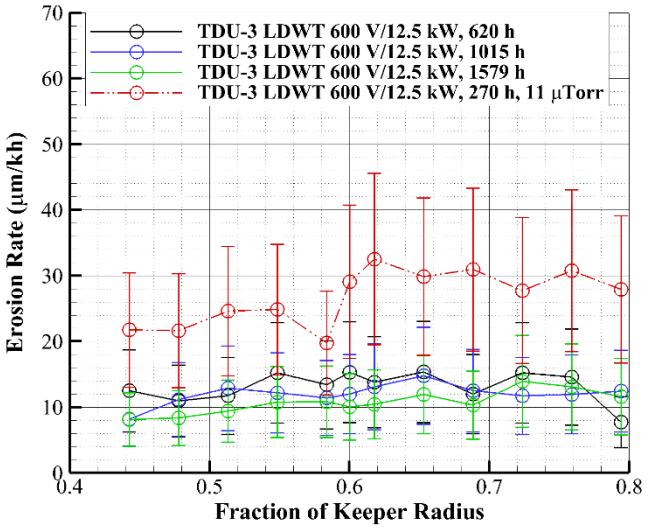

Figure 9. Impact of facility pressure on measured cathode keeper erosion rates for operation at 600 V/12.5 kW.

Acknowledgments

The authors would like to thank Drew Ahern, Maria Choi, Thomas Haag, Wensheng Huang, Jon Mackey, Luis Pinero, Timothy Sarver-Verhey, George Williams, and John Yim also of the Electric Propulsion Systems Branch at NASA GRC for their contributions to the overall success of the LDWT. The authors would also like to thank Scott Hall, Dale Robinson, and Jim Myers of Vantage Partners, LLC for their work, technical input, and guidance as well as Taylor Varouh, Chad Joppeck, Kevin Blake, George Jacynycz, Roland Gregg, Josh Gibson, Matt Daugherty, James Szelagowski, James Zakany, and all of the engineers, technicians, and managers of the Space Environments Test Branch (FTF) for the fabrication, assembly of the test setup, and operation of the vacuum facility. Finally, the authors would like to thank JPL team members Ioannis Mikellides, Vernon Chaplin, Robert Lobbia, Alejandro Lopez-Ortega, and James Polk.

References

[1] Congress, *National Aeronautics and Space Administration Transition Authorization Act of 2017*. 2017.

[2] Smith, B. K., Nazario, M. L., and Cunningham, C. C., "Solar Electric Propulsion Vehicle Demonstration to Support Future Space Exploration Missions," Cleveland, OH, 2012.

[3] Williams, G., Gilland, J. H., Peterson, P. Y., Kamhawi, H., Huang, W., Swiatek, M., Joppeck, C., *et al.*, "2000-hour Wear Testing of the HERMeS Thruster," *52nd AIAA/SAE/ASEE Joint Propulsion Conference*, American Institute of Aeronautics and Astronautics, AIAA Paper 2016-5025, 2016.
doi:10.2514/6.2016-5025

[4] Williams, G. J., Kamhawi, H., Choi, M., Haag, T., Huang, W., Herman, D. A., Gilland, J. H., *et al.*, "Wear Trends of the HERMeS Thruster as a Function of Throttle Point," *35th International Electric Propulsion Conference*, IEPC Paper 2017-207, 2017.

[5] Frieman, J. D., Kamhawi, H., Williams, G. J., Huang, W., Herman, D. A., Peterson, P. Y., Gilland, J. H., et al., "Long Duration Wear Test of the NASA HERMeS Hall Thruster," *2018 Joint Propulsion Conference*, American Institute of Aeronautics and Astronautics, AIAA Paper 2018-4645, 2018.
doi: 10.2514/6.2018-4645.

[6] Peterson, P. Y., Kamhawi, H., Huang, W., Yim, J., Haag, T., Mackey, J., Mcvetta, M., *et al.*, "Reconfiguration of NASA GRC's Vacuum Facility 6 for Testing of Advanced Electric Propulsion System (AEPS) Hardware," *35th International Electric Propulsion Conference*, Electric Rocket Propulsion Society, IEPC Paper 2017-028, 2017.

[7] Frieman, J. D., Liu, T. M., and Walker, M. L. R., "Background flow model of hall thruster neutral ingestion," *Journal of Propulsion and Power*, Vol. 33, No. 5, 2017.
doi: 10.2514/1.B36269.

[8] Byers, D. and Dankanich, J.W., "A Review of Facility Effects on Hall Effect Thrusters," *31st International Electric Propulsion Conference*, Electric Rocket Propulsion Society, IEPC Paper 2009-076, 2009.

[9]Huang, W., Kamhawi, H., and Haag, T., "Facility Effect Characterization Test of NASA's HERMeS Hall Thruster," *52nd AIAA/SAE/ASEE Joint Propulsion Conference*, American Institute of Aeronautics and Astronautics, AIAA Paper 2016-4828, 2016.
doi:10.2514/6.2016-4828.

[10]Huang, W., Kamhawi, H., Loggia, R.B., Brown, D.L., "Effect of Background Pressure on the Plasma Oscillation Chracteristics of the HiVHAc Hall Thruster," *50th AIAA/SAE/ASEE Joint Propulsion Conference*, American Institute of Aeronautics and Astronautics, AIAA Paper 2014-3708, 2014.
doi:10.2514/6.2014-3708.

[11]Frieman, J.D., Kamhawi, K., Mackey, J., Haag, T., Peterson, P.Y., Herman, D.A., Gilland, J., and Hofer, R.R., "Completion of the Long Duration Wear Test of the NASA HERMeS Hall Thruster" *2019 AIAA Propulsion and Energy Forum*, American Institute of Aeronautics and Astronautics, 2019.

[12] Hofer, R. R., Polk, J. E., Sekerak, M. J., Mikellides, I. G., Kamhawi, H., Sarver-Verhey, T. R., Herman, D. A., *et al.*, "The 12.5 kW Hall Effect Rocket with Magnetic Shielding (HERMeS) for the Asteroid Redirect Robotic Mission," *52nd AIAA/SAE/ASEE Joint Propulsion Conference*, American Institute of Aeronautics and Astronautics, AIAA Paper 2016-4825, 2016.
doi:10.2514/6.2016-4825.

[13]Kamhawi, H., Huang, W., Gilland, J., Haag, T., Mackey, J., Yim, J., Pinero, L., *et al.*, "Performance, Stability, and Plume Characterization of the HERMeS Thruster with Boron Nitride Silica Composite Discharge Channel," *35th International Electric Propulsion Conference*, Electric Rocket Propulsion Society, IEPC Paper 2017-392, 2017.

[14]Mikellides, I. G., Katz, I., Hofer, R. R., Goebel, D. M., de Grys, K., and Mathers, A., "Magnetic shielding of the channel walls in a Hall plasma accelerator," *Physics of Plasmas*, 2011, p. 03350.
doi: 10.1063/1.3551583.

[15]Mikellides, I. G., Katz, I., Hofer, R. R., and Goebel, D. M., "Magnetic Shielding of a Laboratory Hall Thruster. I. Theory and Validation," *Journal of Applied Physics*, 2014, p. 043303.
doi: 10.1063/1.4862313.

[16]Mikellides, I., Katz, I., Hofer, R., Goebel, D., de Grys, K., and Mathers, A., "Magnetic Shielding of the Acceleration Channel Walls in a Long-Life Hall Thruster," *46th AIAA/ASME/SAE/ASEE Joint Propulsion Conference & Exhibit*, American Institute of Aeronautics and Astronautics, AIAA Paper 2010-6942, 2010.
doi:10.2514/6.2010-6942.

[17]Snyder, J. S., Baldwin, J., Frieman, J. D., Walker, M. L. R., Hicks, N. S., Polzin, K. A., and Singleton, J. T., "Recommended practice for flow control and measurement in electric propulsion testing," *Journal of Propulsion and Power*, Vol. 33, No. 3, 2017.
doi: 10.2514/1.B35644.

[18]Piñero, L. R., "The Impact of Harness Impedance on Hall Thruster Discharge Oscillations," *35th International Electric Propulsion Conference*, Electric Rocket Propulsion Society, IEPC Paper 2017-023, 2017.

[19]Kamhawi, H., Huang, W., Haag, T., Yim, J., Herman, D., Peterson, P. Y. P. Y., Williams, G., *et al.*, "Performance, Facility Pressure Effects, and Stability Characterization Tests of NASA's Hall Effect Rocket with Magnetic Shielding Thruster," *52nd AIAA/SAE/ASEE Joint Propulsion Conference*, American Institute of Aeronautics and Astronautics, 2016.
doi:10.2514/6.2016-4826

[20]Peterson, P. Y., Kamhawi, H., Huang, W., Williams, G., Gilland, J. H., Yim, J., Hofer, R. R., *et al.*, "NASA's HERMeS Hall Thruster Electrical Configuration Characterization," *52nd AIAA/SAE/ASEE Joint Propulsion Conference*, American Institute of Aeronautics and Astronautics, AIAA Paper 2016-5027, 2016.
doi:10.2514/6.2016-5027.

[21]Frieman, J. D., King, S. T., Walker, M. L. R., Khayms, V., and King, D., "Role of a Conducting Vacuum Chamber in the Hall Effect Thruster Electrical Circuit," *Journal of Propulsion and Power*, Vol. 30, No. 6, 2014, pp. 1471–1479,
doi: 10.2514/1.B35308.

[22]Lobo, M. J., "Electric Propulsion Laboratory | NASA Glenn Research Center," URL: https://www1.grc.nasa.gov/facilities/epl/#facility-overview [cited 8 August 2019].

[23]Yim, J. and Burt, J. M., "Characterization of Vacuum Facility Background Gas Through Simulation and Considerations for Electric Propulsion Ground Testing," *51st AIAA/SAE/ASEE Joint Propulsion Conference*, American Institute of Aeronautics and Astronautics, AIAA Paper 2015-3825, 2015.
doi:10.2514/6.2015-3825.

[24]Yim, J. T., Herman, D. A., and Burt, J. M., "Modeling Analysis for NASA GRC Vacuum Facility 5 Upgrade," NASA Glenn Research Center, Cleveland, OH, NASA/TM 2013-216496, 2013.

[25]Dankanich, J. W., Walker, M., Swiatek, M. W., and Yim, J. T., "Recommended Practice for Pressure Measurement and Calculation of Effective Pumping Speed in Electric Propulsion Testing," *Journal of Propulsion and Power*, 2017, Vol. 33, No. 3, pp. 668–680.
doi: 10.2514/1.B35478.

[26]"Standard Practice for Ionization Gage Application to Space Simulators," ASTM International, West Conshohocken, PA, E296-70, 2015.

[27]Xu, K. G. and Walker, M. L. R., "High-power, Null-type, Inverted Pendulum Thrust Stand," *Review of Scientific Instruments*, Vol. 80, No. 5, 2009, pp. 55103–55103.
doi: 10.1063/1.3125626.

[28]Haag, T. W., "Thrust Stand for High-power Electric Propulsion Devices," *Review of Scientific Instruments*, Vol. 62, No.5, 1991, pp. 1186–1191.
doi: 10.1063/1.1141998.

[29]Pancotti, A., Haag, T., King, S., and Walker, M., "Recommended Practices in Thrust Measurements," *33rd International Electric Propulsion Conference*, Electric Rocket Propulsion Society, IEPC Paper 2013-440, 2013.

[30]Mackey, J., Haag, T. W., Kamhawi, H., Hall, S. J., and Peterson, P. Y., "Uncertainty in Inverted Pendulum Thrust Measurements," *54th AIAA/SAE/ASEE Joint Propulsion Conference*, American Institute of Aeronautics and Astronautics, AIAA Paper 2018-4516, 2018.
doi: 10.2514/6.2018-4516.

[31]Standardization, I. O. for, "ISO 5436-1:2000 Geometrical Product Specifications (GPS) - Surface texture: Profile method; Measurement standards - Part 1: Material measures," 2003.

[32]Mackey, J., Frieman, J. D., Ahern, D. M., and Gilland, J. H., "Uncertainty in Electric Propulsion Erosion Measurements," *2019 Joint Propulsion Conference*, American Institute of Aeronautics and Astronautics, 2019.